Experimental study of the knockout reaction mechanism using ^{14}O at 60 MeV/nucleon

Y. L. Sun,[1] J. Lee,[2,3,*] Y. L. Ye,[1,†] A. Obertelli,[4] Z. H. Li,[1] N. Aoi,[5] H. J. Ong,[5] Y. Ayyad,[5,‡] C. A. Bertulani,[6] J. Chen,[1]
A. Corsi,[4] F. Cappuzzello,[7,8] M. Cavallaro,[7] T. Furono,[9] Y. C. Ge,[1] T. Hashimoto,[5] E. Ideguchi,[5] T. Kawabata,[9] J. L. Lou,[1]
Q. T. Li,[1] G. Lorusso,[2] F. Lu,[10] H. N. Liu,[1,2] S. Nishimura,[2] H. Suzuki,[5] J. Tanaka,[5] M. Tanaka,[5] D. T. Tran,[5] M. B. Tsang,[11]
J. Wu,[1,2] Z. Y. Xu,[12,§] and T. Yamamoto[5]

[1]*State Key Laboratory of Nuclear Physics and Technology, School of Physics, Peking University, Beijing 100871, China*
[2]*RIKEN Nishina Center, 2-1 Hirosawa, Wako, Saitama 351-0198, Japan*
[3]*Department of Physics, The University of Hong Kong, Pokfulam Road, Hong Kong, China*
[4]*CEA, Centre de Saclay, IRFU/Service de Physique Nucléaire, F-91191 Gif-sur-Yvette, France*
[5]*Research Center for Nuclear Physics, Osaka University, Mihogaoka 10-1, Ibaraki, Osaka 567-0047, Japan*
[6]*Department of Physics, Texas A&M University-Commerce, Commerce, Texas 75428-3011, USA*
[7]*INFN - Laboratori Nazionali del Sud, Via S. Sofia 62, I-95125 Catania, Italy*
[8]*Dipartimento di Fisica e Astronomia, Universitá di Catania, Via S. Sofia 64, I-95125 Catania, Italy*
[9]*Department of Physics, Kyoto University, Kyoto 606-8502, Japan*
[10]*Shanghai Institute of Applied Physics, Chinese Academy of Sciences, Shanghai 201800, China*
[11]*National Superconducting Cyclotron Laboratory and Department of Physics and Astronomy, Michigan State University,
East Lansing, Michigan 48824, USA*
[12]*Department of Physics, University of Tokyo, Hongo, Bunkyo-ku, Tokyo 113-0033, Japan*

Background: For the deeply bound one-nucleon removal at intermediate energies using a ^{9}Be or ^{12}C target, a strong reduction of cross section was observed relative to the prediction of eikonal theoretical model. The large disagreement has not been explained and the systematic trend is inconsistent with results from transfer reactions. The recently observed asymmetric parallel momentum distribution of the knockout residue indicates the significant dissipative core-target interaction in the knockout reaction with a composite target, implying new reaction mechanisms beyond the eikonal reaction descriptions.

Purpose: To investigate the reaction mechanism for deeply bound nucleon removal at intermediate energies.

Method: Neutron removal from ^{14}O using a ^{12}C target at 60 MeV/nucleon was performed. Nucleon knockout cross sections were measured. The unbound excited states of ^{13}O were reconstructed by using the invariant mass method with the residues and the associated decay protons measured in coincidence. The measured cross sections are compared with an intra-nuclear cascade (INC) prediction.

Results: The measured cross section of (^{14}O, ^{11}C) is 60(9) mb, which is 3.5 times larger than that of (^{14}O, ^{13}O) channel. This $2pn$-removal cross section is consistent with INC prediction, which is 66 mb with the main contribution being non-direct reaction processes. On the other hand, the upper limit of the cross section for one-neutron removal from ^{14}O followed by proton evaporation is 4.6(20) mb, integrated up to 6 MeV above the proton separation energy of ^{13}O. The calculated total cross section for such reaction processes by the INC model is 2.5 mb, which is within the measured upper limit.

Conclusions: The data provide the first constraint on the role of core excitation and evaporation processes in deeply bound nucleon removal from asymmetric nuclei. The experiment results suggest that non-direct reaction processes, which are not considered in the eikonal model, play an important role in deeply bound nucleon removal from asymmetric nuclei at intermediate energies.

I. INTRODUCTION

Correlation effects play a very important role in the structure of nuclei, which are typical quantum many-body systems. The correlations cause the fractional occupation of single-particle orbits and a spread of the single-particle

strengths over a wide range of excitation energies [1]. The single-particle strength is quantified by spectroscopic factors, which can be deduced from the experimental nucleon-removal cross section, and the correlation effects can be investigated by a reduction factor R_s, which is defined as the experimental-to-theoretical cross-section ratio.

The isospin-asymmetry dependence of reduction factors have been studied by using knockout [2] and transfer [3] reactions with exotic beams, in which the isospin asymmetry is characterized by the difference between the nucleons' separation energies: $\Delta S = S_n - S_p$ for neutron removal or $\Delta S = S_p - S_n$ for proton removal. It has been demonstrated that the benchmark R_s reduction in stable nuclei ($R_s \approx 0.6$–0.7 [4])

---

*jleehc@hku.hk
†yeyl@pku.edu.cn
‡Present address: National Superconducting Cyclotron Laboratory, Michigan State University, East Lansing, Michigan 48824, USA.
§Present address: KU Leuven, Instituut voor Kern-en Stralingsfysica, B-3001 Leuven, Belgium.

can be reproduced by both knockout and transfer reactions (see Refs. [5–7]). However, the trends of reduction factors with asymmetric nuclei from these two methods are not consistent. A significant dependence on ΔS was found for R_s from knockout reactions taken at energies lower than 100 MeV/nucleon with a light composite target (^{9}Be or ^{12}C), which are close to unity for loosely bound nucleons but are as small as 0.24 for deeply bound nucleons [2,8,9]. In contrast, R_s from transfer reactions show a weak dependence on ΔS [3]. Recently, the inclusive knockout reaction with very asymmetric nucleus ^{14}O ($|\Delta S| = 18.6$ MeV) was performed [10] and shows a strong reduction of the deeply bound neutron-removal cross section. The study of ^{14}O(d,t)^{13}O and ^{14}O($d,^3$He)^{13}N transfer reactions, however, indicates that no strong reduction was observed [11]. The structure of ^{14}O ($Z = 8$) could be reasonably described, because it can be reached by the *ab initio* calculations [12–14]. Therefore, these inconsistent results challenges our understanding of deeply bound nucleon-removal mechanisms.

The knockout processes are usually described by the eikonal model, which is formulated by using the sudden and eikonal approximations [15–17]. In the S-matrix calculation of the eikonal model, the knockout residues are treated as a good spectator which can interact at-most elastically with the target. The spectator-core assumption is quite reasonable in describing loosely bound nucleon-removal reactions. On the other hand, non-sudden effects beyond the eikonal model have been observed experimentally which are revealed in the long low-momentum tail [18–21] and the abrupt cutoff [10] at high momentum in the parallel momentum distributions (PMDs) of the residues from the deeply bound nucleon knockout reactions. These deviations from the symmetrical distributions of eikonal predictions can be partly described via a coupled discretized continuum channel (CDCC) calculation [17,22] including higher-order effects or a transfer to continuum (TC) method [10,23]. The applicability of eikonal model for deeply bound nucleon removal is questionable.

Furthermore, non-direct reaction processes such as multiple scattering inside of the projectile and the excitation of the residues might influence the deeply bound nucleon-removal cross section when using a composite target. The eikonal model takes into account the rescattering between the projectile constituents only in an approximate way [24]. Recently, an intranuclear cascade (INC) calculation was performed to calculate the one-nucleon removal cross sections, taking into account three reaction processes including direct knockout, multiple scattering, and nucleon evaporation [25]. Interestingly, the INC could reproduce the deeply bound nucleon-removal cross sections which are largely overestimated by the eikonal model [25]. This work suggests that the excitation and nucleon evaporation of the knockout residues could significantly impact the deeply bound nucleon-removal cross sections. In Ref. [26], the cross sections for the pn and $2pn$ removal from ^{14}O at 305 MeV/nucleon were measured to be 30(6) and 41(6) mb, which were comparable to the one-proton removal channel ($\approx$35 mb) [26]. The large pn- and $2pn$-removal cross sections are expected to receive an non-direct contribution, i.e., after the deeply bound neutron removal from ^{14}O, the residue ^{13}O is non-directly populated to unbound excited states and

decays to lighter isotopes through proton emission. However, until now no such core-excitation effect has been verified experimentally.

The present work aims at studying the one-nucleon removal mechanism from ^{14}O on a carbon target at 60 MeV/nucleon. A coincidence measurement of the knockout residues and the associated decay protons was performed, which allows us to investigate the core excitation strength quantitatively by using the invariant mass method. Exclusive data from this measurement, in addition with the inclusive knockout [10] and transfer [11] results using the same nucleus ^{14}O will provide a benchmark for direct nuclear reaction mechanisms, shedding light on the long-standing intriguing puzzle of the discrepancy between measurements and eikonal-model predictions for knockout reactions involving deeply bound nucleons.

II. EXPERIMENTAL METHOD

The experiment was performed at the Research Center for Nuclear Physics (RCNP) [27], Osaka University. A secondary beam of 60 MeV/nucleon ^{14}O was produced by fragmentation of an 80 MeV/nucleon ^{16}O primary beam on a 2.1-mm-thick Be target. After magnetic-field optimization for the transportation of ^{14}O, the cocktail beam with an intensity of about 7.5×10^3 particles per second was transmitted to a 93 mg/cm^2 secondary C target. The purity of ^{14}O was around 5% with a main contamination of ^{15}O. By adopting an additional time-of-flight (TOF) hardware cut, the triggers from contaminants were partially excluded, giving 24% purity of ^{14}O. The other contaminants (mainly ^{11}C, ^{13}N, and ^{12}N) were separated event by event in the off-line analysis by applying cuts on the TOF and on the energy loss of the ions in the plastic scintillator before the target. Two parallel plate avalanche counters (PPACs) were placed before the target to measure the position and angle of the incoming ^{14}O beam. A schematic view of the experimental setup is given in Fig. 1.

The ejectiles as well as the unreacted ^{14}O beam were detected and identified by a hodoscope [28–30] located 3.8 m downstream from the secondary target. The active area of the hodoscope is 1×1 m^2, consisting of a 5-mm-thick ΔE and two 60-mm-thick E ($E1$, $E2$) plastic scintillators. The ΔE layer is subdivided horizontally into 13 slats, and the $E1$ and $E2$ layers consisted of 16 and 13 scintillator bars set perpendicular to the ΔE slats. The widths of the central five ΔE slats and six $E1$ bars are taken to be narrower (40 mm for ΔE and 38 mm for $E1$) to improve the balance of the counting rate among these scintillators. The widths of the other scintillators in ΔE and $E1$ layer are 100 and 74 mm, respectively. The entire scintillator array was put in rough vacuum to reduce the background reaction with the air. Each plastic scintillator bar was coupled to two photon-multiplier tubes (PMTs) at both ends by light guides and optical pads. Both the timing signal and the charge signal were recorded for each PMT. The TOF of the reaction products was determined by the timing-signal difference between the plastic scintillator in front of the target and the hodoscope. The resolution of the TOF was about 1.7% (sull width at half maximum, or FWHM) extracted from the empty target run. The geometric mean of the charge signals of the two PMTs on the end of scintillator
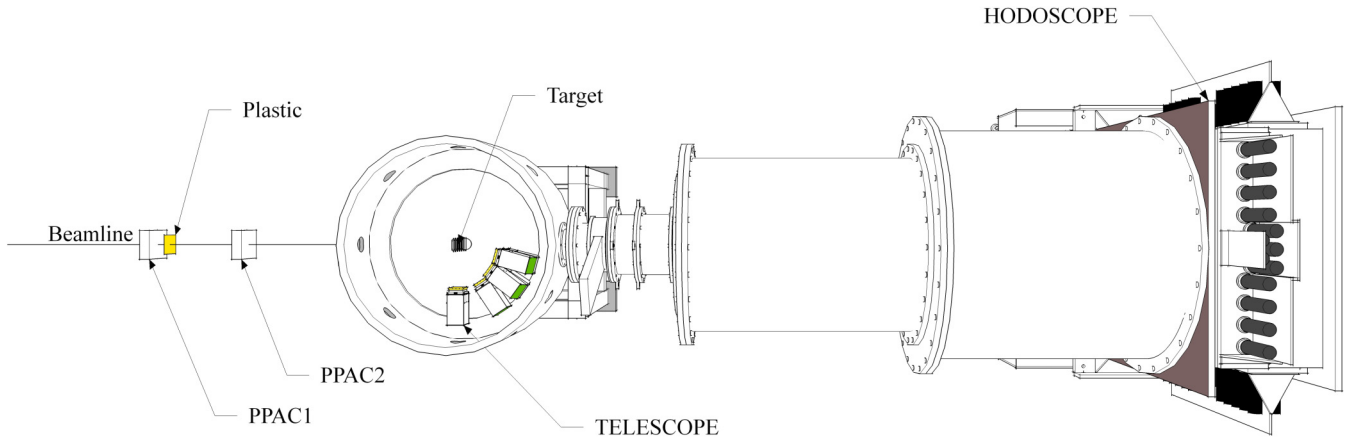
FIG. 1. Schematic view of experimental setup.

bars were used to determine the energy deposit. Meanwhile, the timing difference between each side of the scintillator bars was used to derive the hit position of the reaction products. The position resolutions was deduced to be about 3 cm (FWHM) for both ΔE and $E1$ layer, corresponding to an angular resolution of about $0.2°$.

The momentum vectors of the forward-moving reaction products on the hodoscope were determined by combining their velocities and hit positions. The invariant mass M of a resonance is expressed as

$$M = \sqrt{\left(\sum_i E_i\right)^2 - \left|\sum_i \overrightarrow{P_i}\right|^2},$$ (1)

where E_i and $\overrightarrow{P_i}$ are the energy and momentum of the decay products, respectively. The decay energy is defined as the difference between the invariant mass and the sum of the rest masses of the decay products,

$$E_{\text{decay}} = M - \sum_i M_i.$$ (2)

The resolution of the decay energy and the detector acceptance was obtained by Monte Carlo simulation using the phase-space model [31]. The simulation takes into account the beam size, energy losses in the target, and geometry of the hodoscope. The time and position resolutions of the detectors from the experimental data are also included in the simulation. A few excited states of ^{13}O ranging from 2.7 to 6.1 MeV have been reported previously [32–36]. All excited states of ^{13}O lie above its two-proton separation energy ($S_{2p} = 2.1$ MeV). The one-proton decay product ^{12}N also has no bound excited state [32]. Due to the unfavorable penetrability, the two-proton decay is at least three orders of magnitude less probable than one-proton decay [33]. Therefore, we assume the one-neutron removal from ^{14}O only followed by direct decay to ^{12}N$_{\text{g.s.}}$ and sequential decay through ^{12}N* ($E(2_1^+)$), i.e., ^{13}O$^* \rightarrow p + {}^{12}N_{\text{g.s.}}$ and ^{13}O$^* \rightarrow p + {}^{12}N^*(2_1^+) \rightarrow p + p + {}^{11}$C.

In the simulation, the longitudinal momentum distribution of the residue was calculated by the Goldhaber formula [37], assuming the knocked out neutron has a momentum spread of approximately 210 MeV/c (FWHM) [10]. The simulated acceptance for ^{13}O decaying into two-body ($p + {}^{12}$N) and three-body ($2p + {}^{11}$C) channels is shown in Fig. 2. The events with two different particles hitting the same detector were rejected. As shown in Fig. 2, the two-body and three-body acceptances are 80% and 60% at $E_{\text{decay}} = 0.7$ MeV, respectively, and decrease to about 3% at $E_{\text{decay}} = 10$ MeV.

III. EXPERIMENTAL RESULT

The particle identifications (PIDs) of the fragments for Z and A were performed by applying ΔE-TOF and E-TOF methods, respectively. Figure 3(a) shows the charge number Z identification spectrum of scintillator bars in the middle of ΔE layer. The continuous tail in the low-energy region is mainly caused by the unreacted ^{14}O beams reacting with scintillators. Such background contributions were measured by using the empty target run. Figure 3(b) shows the particle
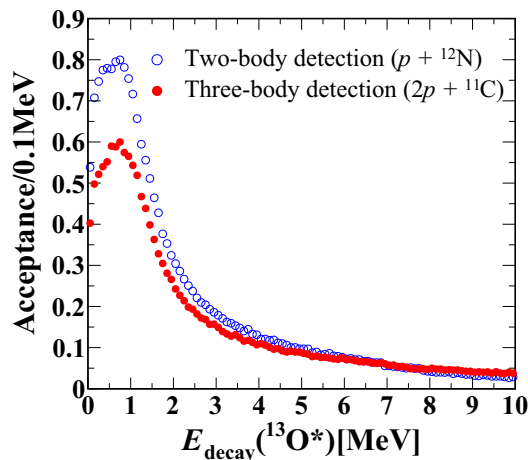

FIG. 2. Two-body and three-body acceptance of hodoscope as a function of decay energy of ^{13}O*. ^{13}O* was assumed to decay to $p + {}^{12}$N$_{\text{g.s.}}$ (open blue circles) or sequentially decay to ^{11}C passing through the intermediate excited state of ^{12}N (filled red circles).
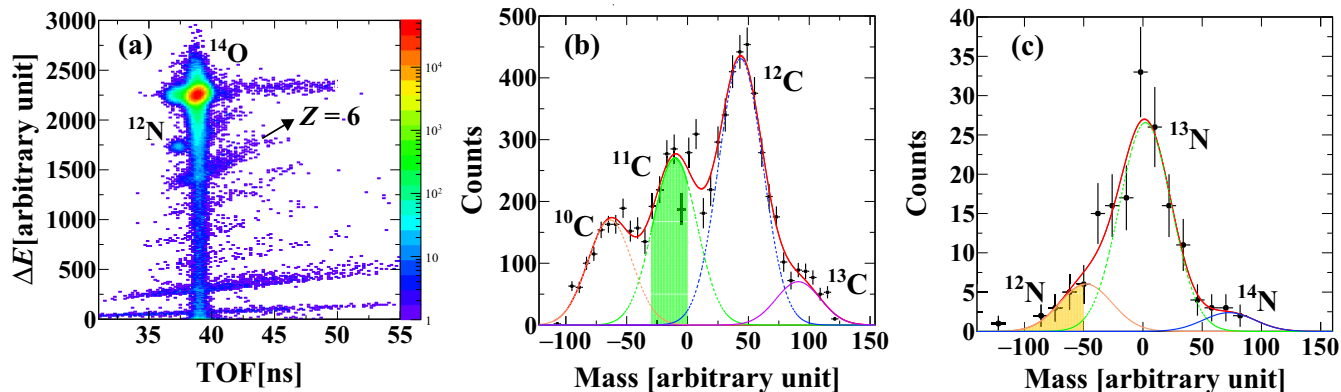
FIG. 3. Particle identification spectrum. (a) The charge number Z identification spectrum for particles after the reaction target. (b) The mass number A identification spectrum for carbon isotopes after the reaction target. The four carbon isotopes are identified as indicated in the figure. The area highlighted in green corresponds to the ^{11}C events included in the present analysis for the decay of ^{12}N* and ^{13}O*. (c) The mass number A identification spectrum for nitrogen isotopes in coincidence with one proton detected at hodoscope. The three nitrogen isotopes are identified as indicated in the figure. The area highlighted in yellow corresponds to the ^{12}N events included in the present analysis for the decay of ^{13}O*. The events within and out of the highlighted area are assumed to have the same invariant mass distribution.

identification spectrum for the carbon isotopes after the background subtraction.

The cross section of $2pn$ removal from ^{14}O was extracted to be 60(9) mb. The isotope spectrum was fit by a multi-Gaussian function with the same width. The statistical uncertainty of the total counts of ^{11}C is 4%. We also performed the automatic fitting without this constraint. The difference was taken as the systematic uncertainty of the cross section of ^{11}C, which is 13.7%. In addition, the quoted uncertainty also includes contributions from the target thickness (0.2%), particle selection (2%), and reaction losses (2%) of the charged particles in the hodoscope. Due to the insufficient energy and TOF resolutions, we could not separate the residue ^{13}O from the unreacted ^{14}O beams. Thus the one-neutron-removal cross section could not be obtained from this measurement. On the other hand, because of the similar beam energy and reaction mechanism, the one-neutron-removal cross section should be almost the same as that measured at 53 MeV/u on a ^{9}Be target, which is 14(1) mb [10]. The measured $2pn$-removal cross section of 60(9) mb is much larger than that of one-neutron removal from ^{14}O, which may be attributed to the core excitations or other complicated reaction processes.

To determine the core excitation strength quantitatively from the pn- and $2pn$-removal channels, it is necessary to investigate the unbound excited states of the residues from $p + {}^{12}$N and $2p + {}^{11}$C channels. It has been reported that the first-excited state of ^{12}N at $E_{\text{decay}} = 0.36$ MeV is strongly populated in the proton knockout and inelastic reactions of ^{13}O on a ^{9}Be target [32]. Thus, the events with one proton and ^{11}C detected in coincidence by the hodoscope were selected and used to reconstruct the decay energy spectrum of ^{12}N according to Eq. (1). The ^{11}C events included in the present analysis for the decay of ^{12}N are highlighted in green, as shown in Fig. 3(b). With this stringent cut, the contamination of ^{10}C and ^{12}C is limited to less than 5%. The ^{11}C events not included in this area are assumed to have the same invariant mass distribution. The background yields of multiplicity-two events determined from the empty target measurement are negligible.

The decay energy spectrum of ^{12}N is shown in Fig. 4(a), in which the peak at 0.36 MeV corresponds to the first-excited state of ^{12}N. The spectrum was fit with a resonant contribution with a Gaussian shape and a nonresonant contribution with a Maxwellian shape, $\sqrt{E_0}\exp(-E/E_0)$. The parameter E_0 was fixed to be 1.06 MeV which was obtained by using the event-mixing technique [38,39]. The width of the peak was
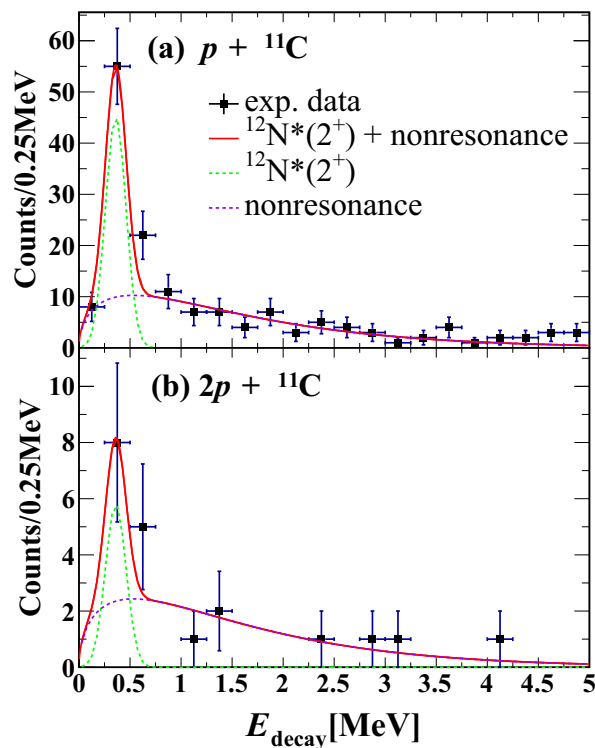

FIG. 4. Decay energy spectrum of ^{12}N*. (a) From p-^{11}C coincidence data. (b) From $2p$-^{11}C triple coincidence data. The solid red curves show the fitting results with a resonant (green dotted line) and a nonresonant contributions (purple dotted line).
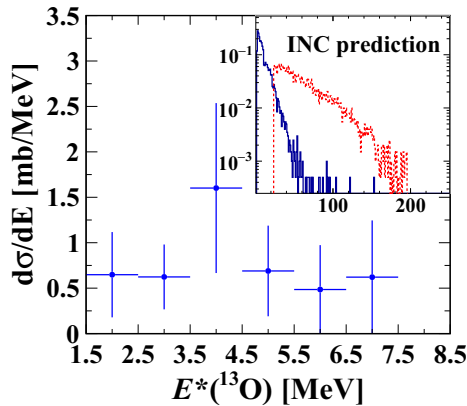
FIG. 5. Excitation energy spectrum of ^{13}O from p-^{12}N and $2p$-^{11}C coincidence measurements using ^{14}O at 60 MeV/nucleon. The inset shows the excitation energy spectrum of ^{13}O predicted by INC model. The contributions from the proton evaporation channels (p-^{12}N and $2p$-^{11}C) (blue solid line) and other decay channels (red dotted line) are shown separately.

deduced to be 0.24(5) MeV (FWHM) which is much larger than the intrinsic width of this state ($\Gamma < 20$ keV [40]). By taking into account the experimental resolutions, the simulated width of this peak was 0.19 MeV which is consistent with the fit value.

By using the same method, the decay energy spectrum of ^{13}O can be reconstructed using $p + {}^{12}$N and $2p + {}^{11}$C coincidence events. Figure 3(c) shows the particle identification spectrum for the nitrogen isotopes in coincidence with one proton detected at hodoscope. The ^{12}N events included in the analysis for the decay of ^{13}O are highlighted in yellow. Due to the limited statistics, no obvious peaks can be observed from the invariant mass spectrum. The low statistics also make it impossible to identify the proton evaporation channels from the angular distribution of the protons in the rest frame of ^{13}O. Assuming that all the coincidence events of $p + {}^{12}$N came from the decay of the excited states of ^{13}O, the upper limit on the cross section of ^{13}O* decaying to $p + {}^{12}$N is 2.0(14) mb. On the other hand, the events of ^{11}C in coincidence with two protons are also scarce. In the triple-coincidence events, the relative kinetic energy of ^{11}C with one of the proton was also reconstructed. Similar to Fig. 4(a), a peak around 0.36 MeV could be observed which corresponds to the first-excited state of ^{12}N, as shown in Fig. 4(b). Thus, the sequential decay through ^{12}N*(2^+) was adopted for the acceptance simulation of $2p + {}^{11}$C triple-coincidence events. With the scarce statistics, we assume that all the coincidence events of $2p + {}^{11}$C came from the decay of the unbound excited states of ^{13}O. The corresponding cross section is 2.6(14) mb. The excitation energy spectrum of ^{13}O after the acceptance correction is shown in Fig. 5. The spectrum is binned in 1 MeV and the contributions from $p + {}^{12}$N and $2p + {}^{11}$C are summed together. For each reaction channel, the average acceptance in the interval of 1 MeV is adopted. The standard deviation of the acceptance within 1 MeV interval is taken as the uncertainty of the acceptance. The integrated cross section up to $E^* = 7.5$ MeV is 4.6(20) mb. The quoted errors

are mainly due to the low statistics and the uncertainties of acceptance.

Here, we note that the excitation of ^{13}O might spread over a large range in energy in this deeply bound nucleon-removal reaction. The observed highest excited state of ^{13}O is the giant dipole resonance located at 8.7 MeV in the pion double charge exchange reaction [36]. More decay channels are available for ^{13}O at higher excitation energies (decay to $3p + {}^{10}$B could happen if $E^* > 10.8$ MeV). These excited states or even continuum states will decay to lighter isotopes such as boron or beryllium. Due to the limitation on detection efficiency, we were not able to observe such high excited states.

In the present work, the measured $2pn$-removal cross section ^{12}C(^{14}O,^{11}C) is 60(9) mb. The upper limit of the cross sections of $p + {}^{12}$N and $2p + {}^{11}$C are 2.0(14) and 2.6(14) mb, integrated from 0 to 6 MeV above the proton separation energy of ^{13}O. In addition, the scaled one-neutron-removal cross section is 16.8(12) mb, which is deduced from the cross section of 14(1) mb at 53 MeV/u [10] multiplied by a factor of 1.2 from the eikonal model taking into account the energy dependence. The eikonal model calculation was performed by using the code MOMDIS [41], which was previously used for the study of the strongly bound neutron removal [8]. The neutron bound-state wave function of ^{14}O was calculated in a Woods–Saxon potential with depth $V_0 = 81.46$ MeV, $r_0 = 2.5$ fm, and $a = 0.6$ fm to reproduce the experimental separation energy $S_n = 23.2$ MeV [42]. In addition, we adopted the ground-state-to-ground-state spectroscopic factor of 3.15 [10,11], which was calculated by using the code OXBASH [43] with the WBT interaction in the $(0 + 2)\hbar\omega$ psd model space.

In the eikonal reaction theory, the one-nucleon-removal cross section is the sum of contributions from the stripping and the diffractive breakup [41]. The stripping mechanism represents the absorption of the removed nucleon by the target, while the diffractive mechanism represents the dissociation of the nucleon from the residue. These two reaction mechanisms are based on the sudden and inert-core approximations, in which the elastic S-matrix of the core and the removed nucleon are calculated by using the nuclear densities and nucleon-nucleon cross section, while the internal structure of the core and the target is not taken into account [41]. In the case of the deeply bound nucleon removal from an asymmetric nucleus, the nucleon separation energies of the residues could be very small, which makes the evaporation channels open more easily. These channels and the separation energy of the core are not explicitly considered in the calculation of eikonal model.

On the other hand, the n- and $2pn$-removal cross sections as well as the cross sections populating the unbound excited states of ^{13}O were calculated by using the INC approach, which takes into account the excitation and evaporation of the knockout residues in a statistical framework. The present INC calculation is based on the Liége Intra Nuclear Cascade (INCL4) [44,45] coupled with the ABLA statistical deexcitation model [46]. In the intranuclear-cascade stage, the collisions between two nuclei are treated as binary cascade collisions between nucleons with energy and momentum conservation [45]. For every collision, Pauli blocking is implemented, allowing only the population of unoccupied final

TABLE I. Summary of cross sections for different exit channels using ^{14}O at 60 MeV/nucleon.

Exit channels	σ_{expt} [mb]	σ_{INC} [mb]	σ_{eik} [mb]
^{13}O	16.8(12)[a]	13	57.6
^{11}C	60(9)	66	Not applicable
^{13}O$^* \rightarrow p + {}^{12}$N	<2.0(14)[b]	0	
^{13}O$^* \rightarrow 2p + {}^{11}$C	<2.6(14)[b]	2.5	
^{13}O$^* \rightarrow$ others	Not measured[c]	3.7	

[a]Deduced from previous measurement in Ref. [10].
[b]For unbound excited states of ^{13}O below 7.5 MeV.
[c]Limited by the geometric acceptance.

states in the phase space. The stopping time of the cascade stage is determined self-consistently, when the variations of the physical quantities (excitation energy, etc.) over time are stable. After the cascade stage, the remnants dissipate by nucleon and light ions emission [46]. The INC model has been proven to be valid for the description of various observables in reactions involving light ions ($A \leqslant 18$) [47].

By using this INC approach, the *n*- and $2pn$-removal cross sections of ^{14}O were calculated to be 13 and 66 mb, respectively. The values are consistent with this work [16.8(12) and 60(9) mb]. From the INC calculation, the direct $2pn$ removal from ^{14}O is negligible and most of the ^{11}C are populated by non-direct reaction processes, such as one-nucleon transfer followed by multinucleon evaporation. Furthermore, the excitation energy spectrum of ^{13}O after one-neutron removal from ^{14}O is also obtained by using the INC model, as shown in the inset of Fig. 5. The spectrum showing no resonant peaks up to 200 MeV, indicates the statistical and nonquantum features of the INC approach. The integral of the spectrum from 1.5 to 200 MeV is 6.2 mb, corresponding to the calculated cross section populating to unbound states of ^{13}O. The predicted low-lying excited states ($E^* < 10$ MeV) of ^{13}O mainly decay to p-^{12}N and $2p$-^{11}C channels with cross sections of 0 and 2.5 mb, respectively. The calculated cross sections are within the upper limits given by this measurement [2.0(14) mb and 2.6(14) mb]. On the other hand, INC also predicts the cross section populating to the higher excited states ($E^* > 10$ MeV) of ^{13}O which mainly decay to other channels such as $3p + {}^{10}$B. The integrated cross section of these channels from 10 to 200 MeV is 3.7 mb, which is comparable to that in the low-lying excited states. The cross sections are summarized in Table I.

In the present work, the upper limit of the cross section for one-neutron removal from ^{14}O followed by proton evaporation is 4.6(20) mb. Our measured upper limit is consistent with the predictions of the INC model of a total cross section of 6.2 mb to unbound excited states of ^{13}O, which cannot be neglected in the deeply bound neutron removal from ^{14}O. In Ref. [25], it has been shown that the one-neutron-removal cross section of ^{14}O could be well reproduced by INC model calculation which gives a reduction factor of around unity. Together with Ref. [25], our results suggest that the large discrepancy involving deeply bound states between measurement and eikonal model calculation could be due to the neglect of non-direct reaction processes in the calculation. However,

we should note that INC models lead to semiquantitative information because they do not explicitly contain structure information. Some invalidity of the INC approach for the one- and multi-nucleon removal reactions was discussed in Refs. [48,49]. On the other hand, significant core excitation in low-lying excited states has been described within the Faddeev-AGS quantum scattering framework [50]. The effects of continuum up to very high excitation energies can be treated using the CDCC formalism, despite the computational difficulty. From the experimental point of view, to reduce the non-direct-reaction processes, we can use a proton target as a cleaner probe for the deeply bound nucleon removal which can be described by the distorted-wave impulse approximation (DWIA) [51].

IV. SUMMARY

In summary, we performed a knockout experiment using 60 MeV/nucleon ^{14}O beam on a carbon target at RCNP. The knockout residues were measured in coincidence with the associated decay protons. The invariant mass method was applied to reconstruct the unbound excited states of ^{13}O. The measured $2pn$-removal cross section is 60(9) mb, which is 3.5 times larger than the deduced one-neutron-removal cross section of 16.8(12) mb. The $2pn$-removal cross section is consistent with the INC prediction, which is 66 mb mainly contributed by the non-direct-reaction processes. On the other hand, the upper limit of the cross section for one-neutron removal from ^{14}O followed by proton evaporation is 4.6(20) mb, integrated up to 6 MeV above the proton separation energy of ^{13}O. The calculated total cross section for such reaction processes by the INC model is 2.5 mb, which is within the measured upper limit. Furthermore, INC predicts a total cross section of 6.2 mb for the non-direct population of unbound ^{13}O*, while the cross section populating the ground state of ^{13}O is only around 16.8 mb. Therefore, the non-direct population of ^{13}O* cannot be neglected in the deeply bound neutron removal from ^{14}O. The experimental results are consistent with INC predictions, indicating that non-direct reaction processes, which are not considered in the eikonal model, play an important role in the deeply bound nucleon removal from asymmetric nuclei at intermediate energies.

ACKNOWLEDGMENTS

[1] W. H. Dickhoff and C. Barbieri, Prog. Part. Nucl. Phys. **52**, 377 (2004).

[2] A. Gade, D. Bazin, B. A. Brown, C. M. Campbell, J. A. Church, D. C. Dinca, J. Enders, T. Glasmacher, P. G. Hansen, Z. Hu, K. W. Kemper, W. F. Mueller, H. Olliver, B. C. Perry, L. A. Riley, B. T. Roeder, B. M. Sherrill, J. R. Terry, J. A. Tostevin, and K. L. Yurkewicz, Phys. Rev. Lett. **93**, 042501 (2004).

[3] J. Lee, M. B. Tsang, D. Bazin, D. Coupland, V. Henzl, D. Henzlova, M. Kilburn, W. G. Lynch, A. M. Rogers, A. Sanetullaev, A. Signoracci, Z. Y. Sun, M. Youngs, K. Y. Chae, R. J. Charity, H. K. Cheung, M. Famiano, S. Hudan, P. O'Malley, W. A. Peters, K. Schmitt, D. Shapira, and L. G. Sobotka, Phys. Rev. Lett. **104**, 112701 (2010).

[4] G. J. Kramer, H. P. Blokb, and L. Lapikás, Nucl. Phys. A **679**, 267 (2001).

[5] B. A. Brown, P. G. Hansen, B. M. Sherrill, and J. A. Tostevin, Phys. Rev. C **65**, 061601(R) (2002).

[6] J. Lee, J. A. Tostevin, B. A. Brown, F. Delaunay, W. G. Lynch, M. J. Saelim, and M. B. Tsang, Phys. Rev. C **73**, 044608 (2006).

[7] B. P. Kay, J. P. Schiffer, and S. J. Freeman, Phys. Rev. Lett. **111**, 042502 (2013).

[8] A. Gade, P. Adrich, D. Bazin, M. D. Bowen, B. A. Brown, C. M. Campbell, J. M. Cook, T. Glasmacher, P. G. Hansen, K. Hosier, S. McDaniel, D. McGlinchery, A. Obertelli, K. Siwek, L. A. Riley, J. A. Tostevin, and D. Weisshaar, Phys. Rev. C **77**, 044306 (2008).

[9] R. Shane, R. J. Charity, L. G. Sobotka, D. Bazin, B. A. Brown, A. Gade, G. F. Grinyer, S. McDaniel, A. Ratkiewicz, D. Weisshaar, A. Bonaccorso, and J. A. Tostevin, Phys. Rev. C **85**, 064612 (2012).

[10] F. Flavigny, A. Obertelli, A. Bonaccorso, G. F. Grinyer, C. Louchart, L. Nalpas, and A. Signoracci, Phys. Rev. Lett. **108**, 252501 (2012).

[11] F. Flavigny, A. Gillibert, L. Nalpas, A. Obertelli, N. Keeley, C. Barbieri, D. Beaumel, S. Boissinot, G. Burgunder, A. Cipollone, A. Corsi, J. Gibelin, S. Giron, J. Guillot, F. Hammache, V. Lapoux, A. Matta, E. C. Pollacco, R. Raabe, M. Rejmund, N. de Séreville, A. Shrivastava, A. Signoracci, and Y. Utsuno, Phys. Rev. Lett. **110**, 122503 (2013).

[12] C. Barbieri, Phys. Lett. B **643**, 268 (2006).

[13] G. Hagen, T. Papenbrock, D. J. Dean, M. Hjorth-Jensen, and B. Velamur Asokan, Phys. Rev. C **80**, 021306(R) (2009).

[14] S. Fujii, R. Okamoto, and K. Suzuki, Phys. Rev. Lett. **103**, 182501 (2009).

[15] C. A. Bertulani and K. W. McVoy, Phys. Rev. C **46**, 2638 (1992).

[16] J. A. Tostevin, J. Phys. G **25**, 735 (1999).

[17] J. A. Tostevin, Nucl. Phys. A **682**, 320 (2001).

[18] Y. Blumenfeld, Ph. Chomaz, N. Frascaria, J. P. Carron, J. C. Jacmart, J. C. Roynette, D. Ardouin, and W. Mittig, Nucl. Phys. A **455**, 357 (1986).

[19] Y. Périer, B. Lott, J. Galin, E. Liénard, M. Morjean, N. A. Orr, A. Péghaire, B. M. Quednau, and A. C. C. Villari, Phys. Lett. B **459**, 55 (1999).

[20] A. Gade, D. Bazin, C. A. Bertulani, B. A. Brown, C. M. Campbell, J. A. Church, D. C. Dinca, J. Enders, T. Glasmacher, P. G. Hansen, Z. Hu, K. W. Kemper, W. F. Mueller, H. Olliver, B. C. Perry, L. A. Riley, B. T. Roeder, B. M. Sherrill, J. R. Terry, J. A. Tostevin, and K. L. Yurkewicz, Phys. Rev. C **71**, 051301(R) (2005).

[21] K. L. Yurkewicz, D. Bazin, B. A. Brown, J. Enders, A. Gade, T. Glasmacher, P. G. Hansen, V. Maddalena, A. Navin, B. M. Sherrill, and J. A. Tostevin, Phys. Rev. C **74**, 024304 (2006).

[22] J. A. Tostevin, D. Bazin, B. A. Brown, T. Glasmacher, P. G. Hansen, V. Maddalena, A. Navin, and B. M. Sherrill, Phys. Rev. C **66**, 024607 (2002).

[23] A. Bonaccorso and D. M. Brink, Phys. Rev. C **38**, 1776 (1988).

[24] R. Crespo, A. Deltuva, and E. Cravo, Phys. Rev. C **90**, 044606 (2014).

[25] C. Louchart, A. Obertelli, A. Boudard, and F. Flavigny, Phys. Rev. C **83**, 011601(R) (2011).

[26] Z. Y. Sun, D. Yan, S. T. Wang, S. W. Tang, X. H. Zhang, Y. H. Yu, K. Yue, L. X. Liu, Y. Zhou, F. Fang, J. D. Chen, J. L. Chen, P. Ma, and C. G. Lu, Phys. Rev. C **90**, 037601 (2014).

[27] T. Shimoda, H. Miyatake, and S. Morinobu, Nucl. Instrum. Methods Phys. Res., Sect. B **70**, 320 (1992).

[28] I. Hisanage, T. Motobayashi, and Y. Ando, RIKEN Accel. Prog. Rep. **31**, 162 (1998).

[29] S. Takeuchi, S. Shimoura, T. Motobayashi, H. Akiyoshi, Y. Ando, N. Aoi, Zs. Fülöp, T. Gomi, Y. Higurashi, M. Hirai, N. Iwasa, H. Iwasaki, Y. Iwata, H. Kobayashi, M. Kurokawa, Z. Liu, T. Minemura, S. Ozawa, H. Sakurai, M. Serata, T. Teranishi, K. Yamada, Y. Yanagisawa, and M. Ishihara, Phys. Lett. B **515**, 255 (2001).

[30] H. Baba, S. Shimoura, T. Minemura, Y. U. Matsuyama, A. Saito, H. Ryuto, N. Aoi, T. Gomi, Y. Higurashi, K. Ieki, N. Imai, N. Iwasa, H. Iwasaki, S. Kanno, S. Kubono, M. Kunibu, S. Michimasa, T. Motobayashi, T. Nakamura, H. Sakurai, M. Serata, E. Takeshita, S. Takeuchi, T. Teranishi, K. Ue, K. Yamada, and Y. Yanagisawa, Nucl. Phys. A **788**, 188 (2007).

[31] R. Brun and F. Rademakers, Nucl. Instrum. Methods Phys. Res., Sect. A **389**, 81 (1997); see also the TGenPhaseSpace class at http://root.cern.ch/

[32] L. G. Sobotka, W. W. Buhro, R. J. Charity, J. M. Elson, M. F. Jager, J. Manfredi, M. H. Mahzoon, A. M. Mukhamedzhanov, V. Eremenko, M. McCleskey, R. G. Pizzone, B. T. Roeder, A. Spiridon, E. Simmons, L. Trache, M. Kurokawa, and P. Navrátil, Phys. Rev. C **87**, 054329 (2013).

[33] B. B. Skorodumov, G. V. Rogachev, P. Boutachkov, A. Aprahamian, V. Z. Goldberg, A. Mukhamedzhanov, S. Almaraz, H. Amro, F. D. Becchetti, S. Brown, Y. Chen, H. Jiang, J. J. Kolata, L. O. Lamm, M. Quinn, and A. Woehr, Phys. Rev. C **75**, 024607 (2007).

[34] P. A. Seidl, M. D. Brown, R. R. Kiziah, C. F. Moore, H. Baer, C. L. Morris, G. R. Burleson, W. B. Cottingame, S. J. Greene, L. C. Bland, R. Gilman, and H. T. Fortune, Phys. Rev. C **30**, 1076 (1984).

[35] P. Couvert, G. Bruge, R. Beurtey, A. Boudard, A. Chaumeaux, M. Garcon, D. Garreta, P. C. Gugelot, G. A. Moss, S. Platchkov, J. P. Tabet, Y. Terrien, J. Thirion, L. Bimbot, Y. Le Bornec, and B. Tatischeff, Phys. Rev. Lett. **41**, 530 (1978).

[36] H. Ward, J. Johnson, K. Johnson, S. Greene, Y. Grof, C. F. Moore, S. Mordechai, C. L. Morris, J. M. O'Donnell, and C. Whitley, Phys. Rev. Lett. **70**, 3209 (1993).

[37] A. S. Goldhaber, Phys. Lett. B **53**, 306 (1974).

[38] Z. H. Yang, Y. L. Ye, Z. H. Li, J. L. Lou, J. S. Wang, D. X. Jiang, Y. C. Ge, Q. T. Li, H. Hua, X. Q. Li, F. R. Xu, J. C. Pei, R. Qiao, H. B. You, H. Wang, Z. Y. Tian, K. A. Li, Y. L. Sun, H. N. Liu, J. Chen, J. Wu, J. Li, W. Jiang, C. Wen, B. Yang, Y. Y. Yang, P. Ma, J. B. Ma, S. L. Jin, J. L. Han, and J. Lee, Phys. Rev. Lett. **112**, 162501 (2014).

[39] Z. H. Yang, Y. L. Ye, Z. H. Li, J. L. Lou, F. R. Xu, J. C. Pei, Z. Y. Tian, K. A. Li, Y. L. Sun, J. Chen, J. Li, W. Jiang, B. Yang, S. D. Chen, Q. Liu, H. L. Zang, J. Feng, and Z. W. Yin, Sci. China: Phys., Mech. Astron. **57**, 1613 (2014).

[40] Evaluated Nuclear Structure Data File (ENSDF); [http://www.nndc.bnl.gov/ensdf/].

[41] C. A. Bertulani and A. Gade, Comput. Phys. Commun. **175**, 372 (2006).

[42] C. A. Bertulani and M. Karakoc, J. Phys.: Conf. Ser. **337**, 012007 (2012).

[43] The computer code OXBASH, B. A. Brown *et al.*, MSU-NSCL Report No. 524.

[44] A. Boudard, J. Cugnon, S. Leray, and C. Volant, Phys. Rev. C **66**, 044615 (2002).

[45] A. Boudard, J. Cugnon, J.-C. David, S. Leray, and D. Mancusi, Phys. Rev. C **87**, 014606 (2013).

[46] A. Kelic, M. V. Ricciardi, and K.-H. Schmidt, in *Proceedings of Joint ICTP-IAEA Advanced Workshop on Model Codes for Spallation Reactions, ICTP Trieste, Italy, 4–8 February (2008)*,

edited by D. Filges, S. Leray, Y. Yariv, A. Mengoni, A. Stanculescu, and G. Mank (IAEA, Vienna, 2008), INDC(NDS)-530, pp. 181–221.

[47] D. Mancusi, A. Boudard, J. Cugnon, J.-C. David, P. Kaitaniemi, and S. Leray, Phys. Rev. C **90**, 054602 (2014).

[48] L. Audirac, A. Obertelli, P. Doornenbal, D. Mancusi, S. Takeuchi, N. Aoi, H. Baba, S. Boissinot, A. Boudard, A. Corsi, A. Gillibert, T. Isobe, A. Jungclaus, V. Lapoux, J. Lee, S. Leray, K. Matsui, M. Matsushita, T. Motobayashi, D. Nishimura, S. Ota, E. C. Pollacco, G. Potel, H. Saku-rai, C. Santamaria, Y. Shiga, D. Sohler, D. Steppenbeck, R. Taniuchi, and H. Wang, Phys. Rev. C **88**, 041602(R) (2013).

[49] D. Mancusi, A. Boudard, J. Carbonell, J. Cugnon, J.-C. David, and S. Leray, Phys. Rev. C **91**, 034602 (2015).

[50] R. Crespo, A. Deltuva, and A. M. Moro, Phys. Rev. C **83**, 044622 (2011).

[51] K. Ogata, K. Yoshida, and K. Minomo, Phys. Rev. C **92**, 034616 (2015).